Crosshole electromagnetic tomography: A new technology for oil field characterization

By MICHAEL WILT
Lawrence Berkeley Laboratory

KIHA LEE
Lawrence Livermore National Laboratory

DAVID ALUMBAUGH
Sandia National Laboratory

H.F. MORRISON, ALEX BECKER and HUNG-WEN TSENG
University of California-Berkeley

CARLOS TORRES-VERDIN
Schlumberger Doll Research

With the advent of crosshole seismic technology in the 1980s a new generation of high resolution geophysical tools has become available for reservoir characterization. The chief improvement is simply that the tools are deployed in boreholes so measurements take place much closer to the region of interest.

We have developed a low frequency crosshole electromagnetic system capable of imaging electrical resistivity in oil fields at borehole separations up to 1 km. Low frequency crosshole EM results yield different and very complementary reservoir data as compared to seismic. Whereas seismic velocity and attenuation is more sensitive to variations in rock matrix, the electrical resistivity distribution, derived from EM data, is more sensitive to variations in rock pore fluid.

Electrical resistivity depends directly on porosity, pore fluid resistivity, and saturation -all key parameters in reservoir characterization. Combined with other information in any of these parameters, resistivity yields increased accuracy in the others. For example, in well logging, porosity values are combined with resistivity and some knowledge of pore water resistivity to yield water saturation. Even without this information, interwell resistivity data are valuable for determining boundaries, mapping variations in reservoir properties, and, in general, mapping interwell heterogeneity. Another important application is EOR monitoring. Whereas seismic velocity variations during steam flooding are on the order of 10%, resistivity variations are as much as an order of magnitude.

Crosshole EM systems were developed for tunnel detection and other hard rock applications in the early 1970s at Lawrence Livermore National Laboratory (LLNL). These were high frequency systems (>20 MHz) using electric dipole antennas and were designed to use ray tomography for data interpretation. In the "soft rock" oil field environment, high frequency signals cannot propagate for more than a few meters due to the low power of the poorly coupled system and the severe attenuation caused by the low resistivity elastic section. At frequencies in the kilohertz range it is possible to build powerful borehole tools to propagate signals up to 1 km through a typical oil field section. The penalty is that at low frequencies the EM signals are diffusive in nature and traditional ray tomography is not applicable. Therefore new tools must be developed for interpreting the data.

Based on theoretical developments in the 1980s researchers at Lawrence Berkeley Laboratory (LBL), LLNL, and the University of California-Berkeley began joint research on the problem of data collection and imaging in low frequency crosshole EM. This research was sponsored by the Department of Energy and a consortium from the oil, minerals, environmental and oil field service industries.The crosshole EM induction system was designed to be an extension of the borehole induction logs into the region between wells. The system, in fact, operates in a very similar fashion to a logging tool with the transmitter and receiver sections deployed in separate boreholes.

Instrumentation and deployment. One of our first objectives was to test the concept in field trials as early as possible. For this reason instrumentation was kept very simple; off the shelf components were used whenever possible.

With the first transmitter configuration, we generated high power AC signals at the surface and sent them down standard logging cable to be broadcast using a vertical axis tuned coil (Figure 1). The borehole coil consists of a magnetically permeable core (Mumetal or ferrite) wrapped with 100-300 turns of wire and tuned with a capacitor. The coil is tuned to broadcast a single frequency; we can modify this frequency by changing the number of turns (inductance) and/or capacitor in the tool. This is an important benefit because the

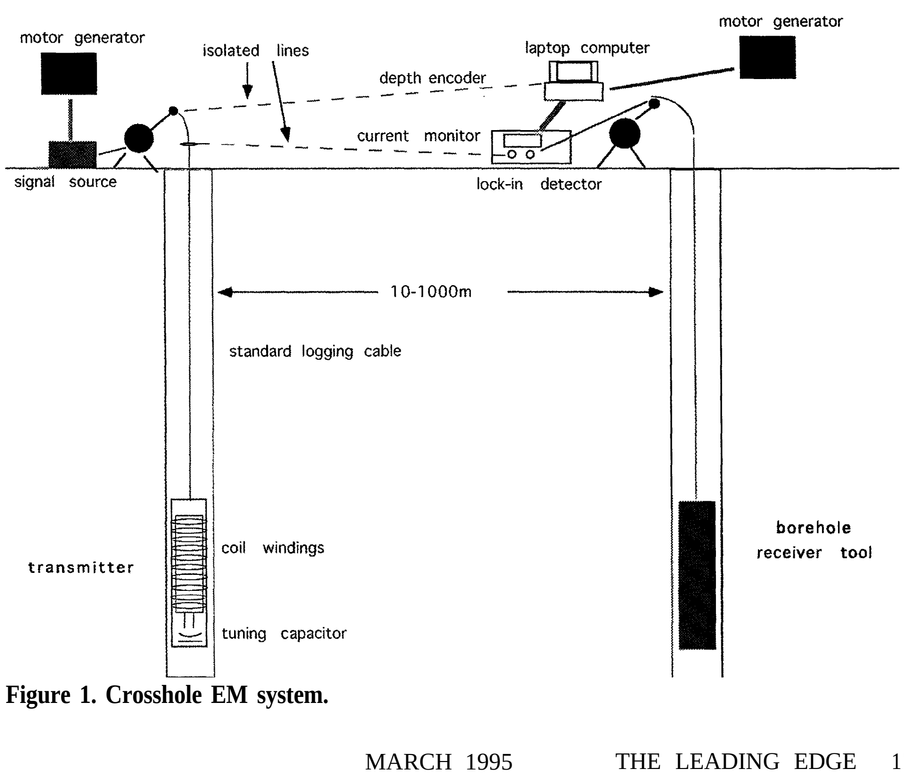

Figure 1. Crosshole EM system.

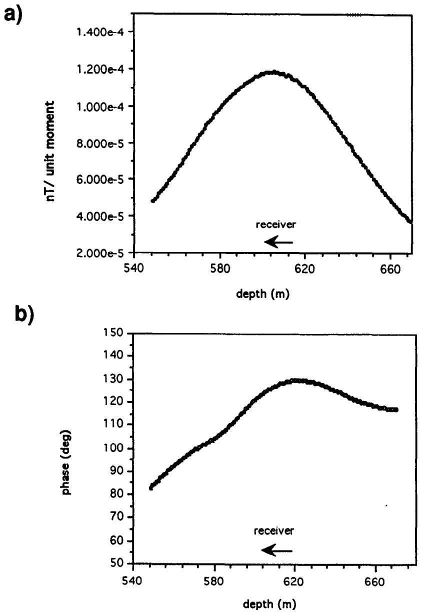

Figure 2. Sample crosshole EM data profile.

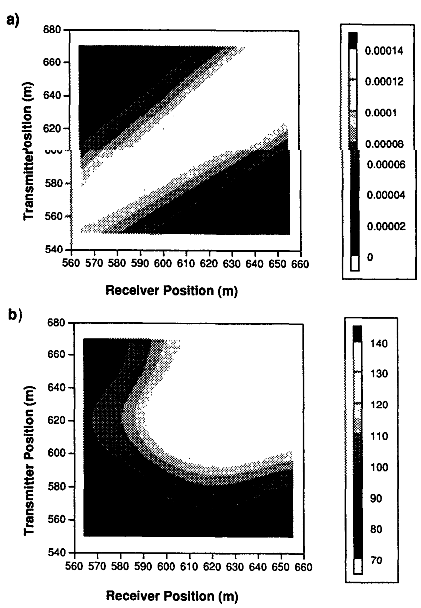

Figure 3. Crosshole EM data set from Devine, Texas. (a) Amplitude, (b) phase.

optimum operating frequency depends on borehole separation and background resistivity. Too low a frequency limits the resolution, too high limits the range. Using this concept, we have operated in a variety of fields at borehole separations of 10-300 m using frequencies of 40 Hz- 100 kHz.

The receiver station is equally simple. Vertical magnetic fields are detected with a commercial borehole coil and the signal is transmitted up the logging cable for measurement with a commercial lock-in detector. We use a measurement of the transmitter current as the phase reference signal for the lock-in so we are directly coupled to the transmitted signal. This signal is carried to the receiver using an optically isolated line. Wheel type encoders are used to keep track of tool depths and a portable computer is used to log the data.

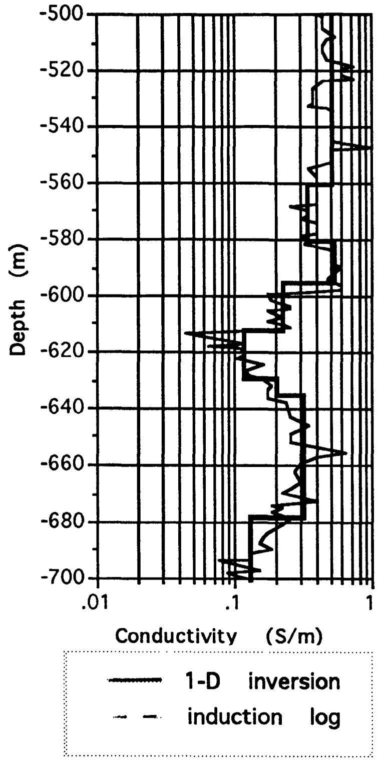

Figure 4. Comparison of layered model interpretation from EM data and borehole induction log at Devine.

With this simple analog system we have been able to collect high quality data, typically repeatable and reciprocal to one percent. We believe the high quality is due to careful attention to isolation and local grounding of the transmitter and receiver sections. Each unit has a separate generator for power supply, a local common ground and communications between the units are conducted using optically isolated cables.

Our initial field test was conducted at the British Petroleum test facility in Devine, Texas, in October 1990. We deployed our system in essentially flatlying geology using two 1000 m deep fiberglass cased boreholes located 100 m apart. The EM system is deployed by keeping the receiver coil stationary in one borehole while moving the transmitter in the other hole. Magnetic fields, transmitter current and corresponding depth measurements are made as the transmitter traverses the desired segment of the borehole; an example of these data is given in Figure 2. A similar profile to Figure 2 is collected for different receiver depths until the desired interval is covered by both transmitter and receiver positions. For a typical crosshole survey we measure from 16-20 receiver profiles covering a depth interval of between 100 m and 200 m.

Figure 3 shows contour plots from the Devine experiment with data from individual profiles plotted at the source and receiver positions. Amplitude data dominantly reflect the relative positions of the source and receiver coils, peaking where the coils are closest. Phase data are less dependent upon source-receiver separation and more closely reflect the geology. The contours are seamless plots that show higher peak amplitudes and lower phase rotation in the higher resistivity limestone beds deeper in the section. In the lower resistivity sands and shales in the upper parts of the section, amplitude attenuation and phase rotation are greater. Note that the average resistivity of the section is less than 5 ohm-m and the depth is approximately 600 m.

Figure 4 compares a layered model, derived by fitting the Devine data in Figure 3 with a least-squares inversion code, to a borehole induction log from one of the tomography wells. There is remarkable correspondence between the two plots at this highly stratified site. This figure illustrates the resolution achievable with crosshole EM and also that the resistivity derived from borehole logs may be useful in constraining interpretation at more complex sites.

Magnetic field data (Figure 3) are directly useful only as indicators of data quality. To effectively use them, we must apply EM modeling to obtain the resistivity distribution between boreholes; this is where things get difficult. The general three-dimensional EM problem is too difficult and computer intensive for routine use; we therefore have applied approximate methods for forward solutions and have fit the measured data using well established least squares inversion techniques.

The first solution that we developed assumes cylindrical symmetry and the Born approximation (low contrast scattering). The second code assumes a two-dimensional rectangular geometry and more general low contrast assumption. Full three-dimensional solutions have recently been developed but parallel computers are required for routine data interpretations.

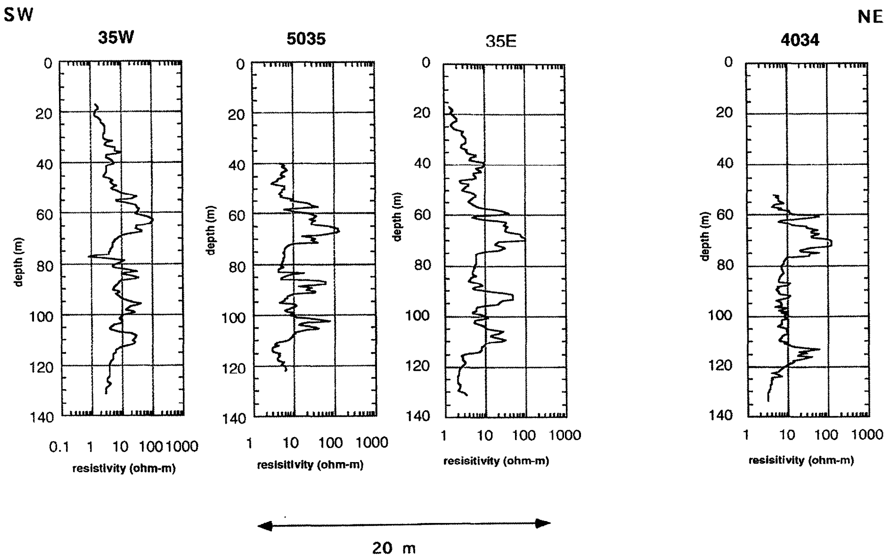

Figure 5. Northeast-southwest resistivity cross section derived from borehole induction logs in a central California oil field.

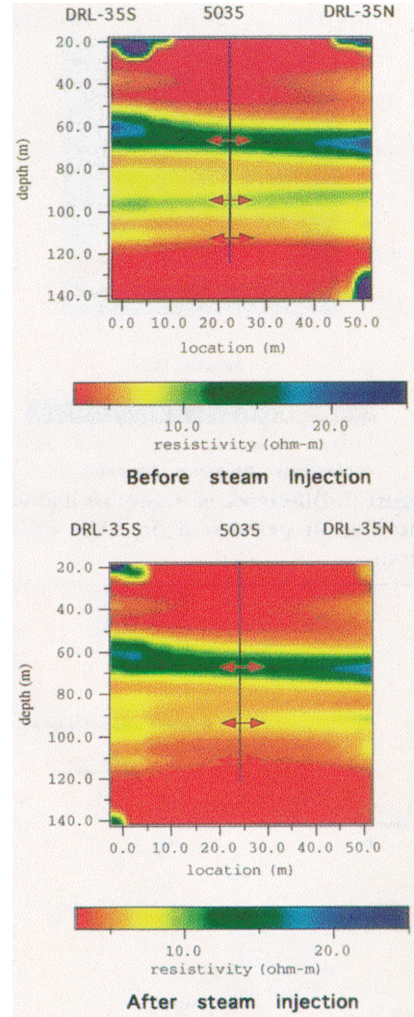

Figure 6. Resistivity image from crosshole EM data for central California oil field (a) before and (b) after steam injection.

Steam flood monitoring. Heavy oil has been produced with the aid of steam injection from shallow unconsolidated sands in the San Joaquin Valley of central California for years. Although most thermal EOR projects have been economically successful, many have problems with steam override, steam bypass, and inefficient sweep due to channeling. Developing low cost geophysical monitoring methods for EOR has been a priority of operating companies for some time. Seismic techniques have been applied with good success but many developers are reluctant to use them due to the high cost of drilling dedicated observation wells and the cost of surveys. Crosshole EM is an excellent method for monitoring a steam drive due to the high sensitivity of resistivity to changes in temperature and steam saturation. Induction logging measurements in oil fields undergoing EOR have shown that resistivity typically decreases from 35 to more than 80% after steam injection. This is due to the increase in temperature as well as the replacement of high resistivity oil by lower resistivity salt water and steam. The corresponding change in seismic velocity is 10-12%.

Mobil has operated several EOR projects in central California and we have been involved in applying crosshole EM technology as a pilot test in one. For this experiment, two fiberglass-cased observation wells were drilled along a northeast-southwest profile near a steam injector in shallow heavy oil sands. The wells were drilled for the combined purposes of crosshole EM surveys and repeated temperature and induction logging. The injection well was completed to inject steam at depths or 65, 90 and 120 m, into upper, middle and lower members of the target oil sand. The steam injection is expected to follow the natural northwest-southeast fracture pattern and the plume is expected to develop as an ellipse with the major axis aligned with the natural fractures. The crosshole EM data can therefore be expected to roughly follow the assumption of two-dimensional rectangular geometry. Crosshole EM measurements were made at a frequency of 5 kHz before steaming and then six months after the onset of steaming.

Figure 5 shows a cross-section derived from borehole induction logs in this section of the field. The higher resistivity intervals typically represent oil sands; the lower resistivity units are confining silts and shales. The target sands extend 60-120 m in three separate intervals. The upper sand, which has a thickness of up to 20 m, has the highest resistivity and is the most continuous of the three. This is the thickest of the three members and it dips gently eastward at about 6 degrees. The middle and lower members are thinner and less continuous. The middle member seems to "pinch-out" at the western well and "water-out" at the eastern well.

Before and after crosshole resistivity images near the steam injection well are shown in Figure 6a,b. Bluer sections represent higher resistivity zones associated with heavy-oil sands; red areas are lower resistivity silts and confining shale beds of l-8 ohm-m, with an average value of 3 ohm-m. The water table lies at a depth of 130 m. The initial image clearly shows the upper oil sand and less clearly the middle and lower sands. This is consistent with borehole logs which indicate that the lower sands are less continuous.

After steaming, the resistivity image is visibly different only at depths below 70 m in the center of the image, where the bluish region associated with the middle and lower target sands fades (i.e., becoming lower in resistivity) especially near the steam injector. In all other parts of the image the results are similar and in areas above the oil reservoir the before and after data agree to within a few percent.

Figure 7 shows a difference image made by subtracting the two previous images. A substantial steam chest has formed in the middle and lower sands and almost none of the steam has gone into the upper oil sand. The steam also seems to preferentially flow to the east. This is in accord with the induction logs, which indicate that the lower sands are better connected eastward than westward. It is also consistent with increased production in well 4034.

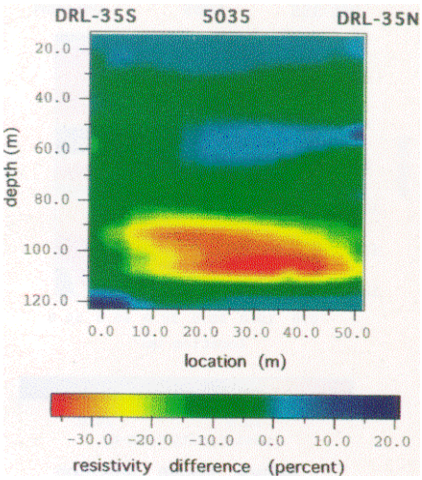

Figure 7. Difference of Figure 6a and 6b, showing the position of the EOR steam chest.

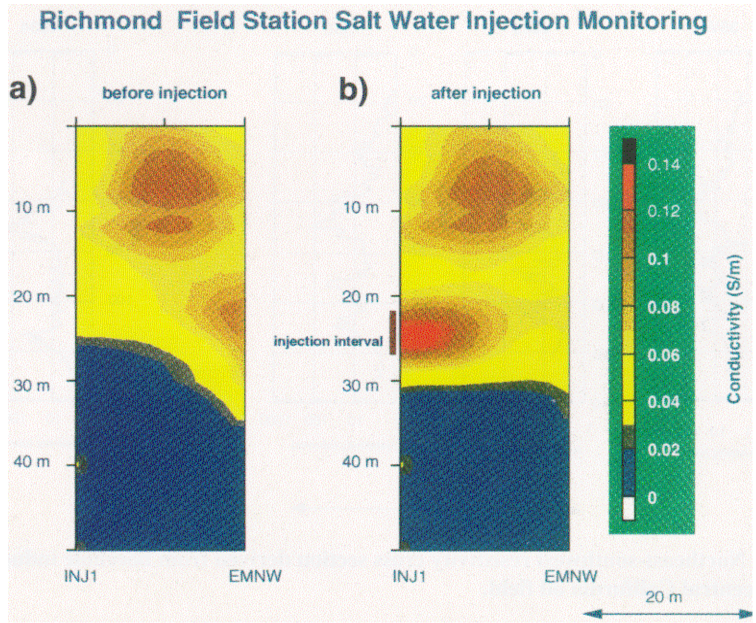

Figure 10. Resistivity cross sections between wells INJ1 and NW (a) before and (b) after salt water injection.

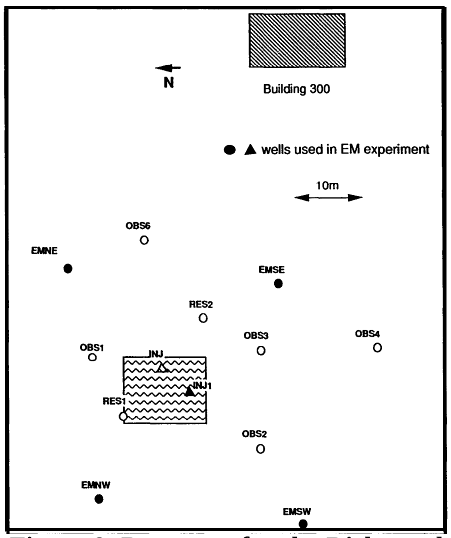

Figure 8. Base map for the Richmond Field Station salt water injection experiment.

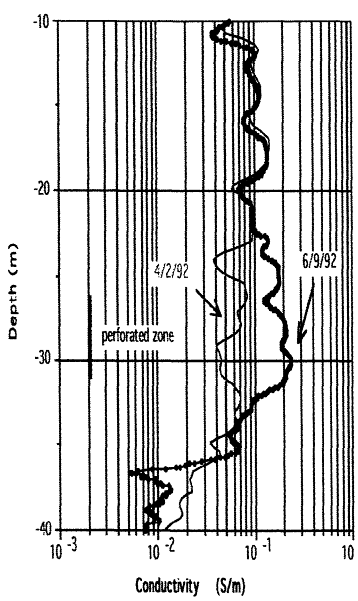

Figure 9. Borehole induction logs from INJ1 before and after salt water injection.

Salt water injection monitoring. Although both seismic and EM methods are effective for imaging changes due to a steam flood, a water flood is a different story. Electrical resistivity is a strong function of water salinity, whereas to seismic velocity it is virtually transparent. If the injected flood has a different salinity than native groundwater and oil, it should be readily detected with EM measurements.

Our second field example is a salt water injection monitoring experiment at the University of California Richmond Field station, 7 km north of the Berkeley campus. The experiment was designed to be a scale model depiction of a water flood as commonly used in the oil business or a full scale simulation of an environmental water contamination problem. With appropriate permission from the water agencies, we located a suitable aquifer and injected and withdrew a salt water slug, collecting crosshole EM data before and after injection and withdrawal.

In contrast to the other two sites, the geology at Richmond is a complex configuration of muds, silt, and gravels overlying a discontinuous basal unit of sandstone (or shale). We drilled four plastic-cased observation wells symmetrically arranged about a central injector (Figure 8). The wells are drilled to a depth of 60 m and perforated in a producing gravel layer at 30 m.

We designed the experiment such that the injection well would be used for both salt water injection and deployment of the transmitter tool. The other wells would be used for crosshole EM measurements, repeat logging and water level measurements. Salt water was prepared by mixing city water and salt in a pond until a uniform water conductivity of 1 S/m was achieved. We injected 250 000 liters of salt water, in total, at a rate of 40 liters/minute into well INJ1 over a period of three days.

Figure 9 shows borehole induction logs from well INJ1 before and after injection. From a depth of 23-31 m, the logs show that conductivity has increased (resistivity has decreased) substantially due to salt water injection. The before and after logs show a mirror image: the higher resistivity sands and gravels before injection have become the lower resistivity units after injection. The largest decrease is between 26 and 30 m where the well is perforated; here resistivity has changed from 15 to 3.5 ohm-m.

The injected salt water body is a relatively small feature that requires a three-dimensional EM inversion for data interpretation. Fortunately the salt water flood has a first-order cylindrical symmetry about the injection and transmitter borehole INJ1. We can therefore develop images for the planes corresponding to the four receiver wells separately, using our 2-D cylindrically symmetric code, and later apply a more sophisticated code to assure that this ap roach is valid.

Figure 10 shows conductivity images for EMNW before and after injection. The preinjection image, Figure 10a, shows a conductive overburden overlying a more resistive basement. This is consistent with

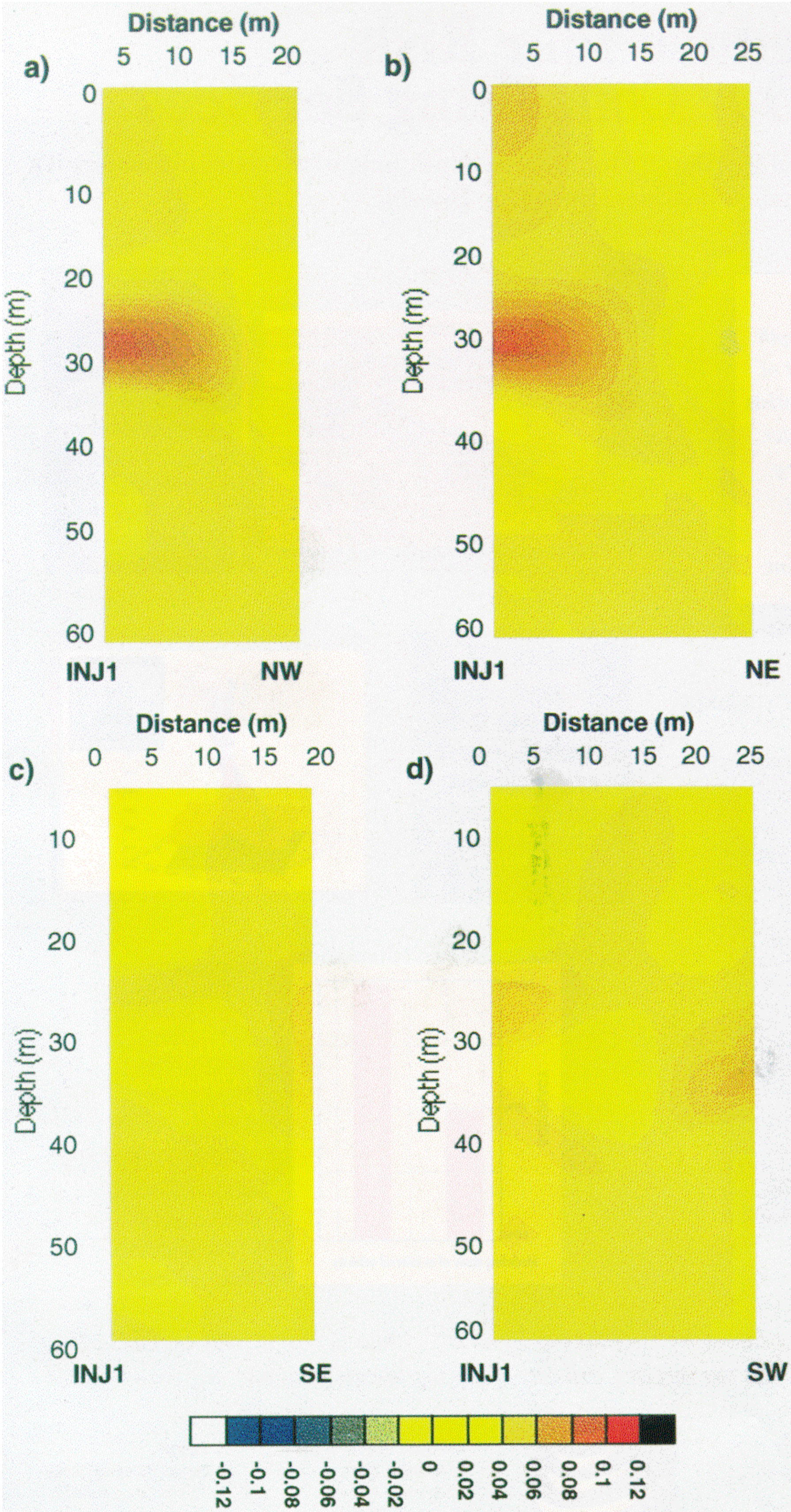

Figure 11. Resistivity differences before and after salt water injection for the five-spot well pattern.

the borehole induction logs. The postinjection image (Figure 10b) clearly shows a region of high conductivity at 30 m that is not present prior to injection. This anomaly corresponds to the permeable sand intersected at the injection zone and strongly suggests that salt water has migrated within this sand to the northwest. Images of the EMNE data indicate some migration to the northeast while the EMSW and EMSE results indicate almost no migration to the southeast or southwest. This interpretation is consistent with an earlier salt water injection monitoring experiment at Richmond using the dc resistivity method.

The direction of plume migration becomes more apparent if we plot the change in conductivity between the before and after images. This is a simple process of subtracting the conductivities in the preinjection image from those in the postinjection image on a cell by cell basis. Figure 11 shows a large conductivity increase between INJ1 and both of the northern wells. The fact that the magnitude of the changes in the EMNW well is slightly greater than those in the EMNE well suggests that the water might be moving preferentially in this direction. To the south the changes are much smaller in magnitude and indicate a conductivity decrease. This implies that little of the injected water is migrating in this direction.

Conclusions. Subsurface conductivity imaging is practical with crosshole EM induction. Although there are a number of petroleum and environmental applications that can benefit from this level of resolution now, the method is still in its infancy and we can expect higher data quality and higher resolution imaging in the future.

In the near term we can expect significant advances in both hardware and software. Single frequency downhole oscillators are presently under development and a multifrequency transmitter is not too far behind. Several groups are working on borehole transient systems although these are by nature more difficult to engineer. Imaging software is under development at several research laboratories (LLNL, LBL, Sandia National Laboratory, and Schlumberger-Doll Research); many of these newer codes are designed to handle the high contrast anomalies and make use of multifrequency or transient data. LE